Three-Dimensional Evolution of Water Vapor Distributions in the Northern Hemisphere Stratosphere as Observed by the MLS

W. A. LAHOZ,* A. O'NEILL,* E. S. CARR,† R. S. HARWOOD,† L. FROIDEVAUX,# W. G. READ,# J. W. WATERS,# J. B. KUMER,@ J. L. MERGENTHALER,@ A. E. ROCHE,@ G. E. PECKHAM,& AND R. SWINBANK**

*Centre for Global Atmospheric Modelling, Department of Meteorology, University of Reading, Reading, United Kingdom
†Department of Meteorology, University of Edinburgh, Edinburgh, Scotland
#Jet Propulsion Laboratory, California Institute of Technology, Pasadena, California
@Lockheed Palo Alto Research Laboratory, Palo Alto, California
&Department of Physics, Heriot-Watt University, Edinburgh, Scotland
**The Meteorological Office, London, Bracknell, Berkshire, United Kingdom

(Manuscript received 21 March 1994, in final form 13 July 1994)

ABSTRACT

The three-dimensional evolution of stratospheric water vapor distributions observed by the Microwave Limb Sounder (MLS) during the period October 1991–July 1992 is documented. The transport features inferred from the MLS water vapor distributions are corroborated using other dynamical fields, namely, nitrous oxide from the Cryogenic Limb Array Etalon Spectrometer instrument, analyzed winds from the U.K. Meteorological Office (UKMO), UKMO-derived potential vorticity, and the diabatic heating field. By taking a vortex-centered view and an along-track view, the authors observe in great detail the vertical and horizontal structure of the northern winter stratosphere. It is demonstrated that the water vapor distributions show clear signatures of the effects of diabatic descent through isentropic surfaces and quasi-horizontal transport along isentropic surfaces, and that the large-scale winter flow is organized by the interaction between the westerly polar vortex and the Aleutian high.

1. Introduction

With the launch of the *Upper Atmosphere Research Satellite (UARS)* on 12 September 1991 (Reber 1993), a wealth of three-dimensional global datasets has become available. The *UARS* dataset (see, e.g., *UARS* special issue of *Geophysical Research Letters,* Vol. 20, 1993) contains simultaneous measurements of a suite of important geophysical parameters such as temperature, ozone, species involved in the destruction of ozone (e.g., chlorine monoxide), and chemical tracers (e.g., water vapor and nitrous oxide).

As part of the *UARS* project, a data assimilation system has been developed by the U.K. Meteorological Office (UKMO). The UKMO data assimilation system produces global analyses of temperatures, winds, geopotential heights, and vertical velocities that have uniformly good resolution (Swinbank and O'Neill 1994). The availability of *UARS* data and UKMO analyses provides an unprecedented opportunity to carry out detailed studies of transport in the middle atmosphere. The need for such studies has been highlighted by the recent discoveries of severe Antarctic ozone depletion (Farman et al. 1985) and the potential for depletion in the Northern Hemisphere (e.g., Waters et al. 1993). In particular, there is now an unprecedented opportunity to carry out transport studies of the winter stratosphere in a physically oriented basis.

The dominant feature of the stratospheric circulation in winter is a cold westerly vortex centered near the pole and extending from the lower stratosphere into the mesosphere. An associated feature is the quasi-stationary Aleutian anticyclone, which tends to lie over the date line. The polar vortex undergoes a pronounced seasonal cycle, growing steadily in early winter, weakening rapidly in late winter, and finally disappearing in spring. By virtue of its longevity and (partial) resilience to disturbances, the polar vortex tends to organize the large-scale flow in the stratosphere, tending to align isopleths of tracer gas mixing ratios along streamlines.

In the past, the theory underpinning transport studies in the northern winter stratosphere has been based on a wave–mean flow interaction picture (see, e.g., Andrews et al. 1987). However, in view of the asymmetry of the northern winter stratosphere, the appropriate picture in which to view the seasonal evolution of the northern winter stratosphere is a vortex-centered view, that is, a coordinate-independent picture, where one focuses on the evolution of the large-scale flow and tracer distributions with respect to the westerly polar vortex.

Corresponding author address: Dr. W. A. Lahoz, CGAM, Department of Meteorology, University of Reading, Reading RG6 2AU, United Kingdom.

In this paper we study the evolution of water vapor in the stratosphere of the Northern Hemisphere during winter 1991/92. In the stratosphere water vapor behaves as a conserved tracer (Brasseur and Solomon 1984). Water vapor concentrations are derived from measurements made by the Microwave Limb Sounder (MLS) aboard *UARS*. To corroborate the measurements from MLS, another conserved tracer will be used, namely, nitrous oxide as observed by the Cryogenic Limb Array Etalon Spectrometer (CLAES) instrument aboard *UARS*. Corroboration with CLAES water vapor measurements is not undertaken, as at present this dataset is not as mature as the MLS water vapor or CLAES nitrous oxide datasets.

The aim of this paper is to document and interpret the evolution of the MLS water vapor concentrations in and around the stratospheric polar vortex. The period studied is 26 October 1991 to 19 July 1992. In section 2 we describe the datasets used in this study. In section 3 we document the structure and evolution of water vapor mixing ratios, which will be compared with that of nitrous oxide as measured by CLAES. The structure of the tracer fields will be interpreted by reference to the distribution of winds and potential vorticity derived from UKMO analyses and to diabatic heating rates calculated from MLS data. Section 4 presents conclusions.

2. Data

The MLS water vapor is measured by a 183-GHz radiometer, which was built in the United Kingdom (Barath et al. 1993). The measurements have a horizontal resolution along the viewing track of approximately 400 km and a vertical resolution of 4 km. The latest version of the data (V0003) is generally of good quality at all latitudes in the pressure range 0.2–20 hPa (Lahoz et al. 1994). Between about 25 and 50 hPa these data can be biased toward climatology (larger values) under dehydrated conditions such as occur in the Antarctic polar vortex, and below 50 hPa are increasingly biased toward climatology at all latitudes. The MLS water vapor climatology (Remsberg et al. 1989) consists mainly of monthly zonal means from the Limb Infrared Monitor of the Stratosphere (LIMS). The present study is limited to the pressure range 2–20 hPa, where the estimated precision of individual water vapor measurements (i.e., in an along-track view) is approximately 0.2 parts per million by volume (ppmv) and the estimated accuracy is about 15%.

Nitrous oxide is measured by the CLAES instrument (Roche et al. 1993). The measurements have a horizontal resolution along the viewing track of approximately 400 km and a vertical resolution of 2.5 km. The latest version of the data (V0006) is regarded as reliable for stratospheric levels above 50 hPa for latitudes poleward of 40°N, and for stratospheric levels above 10 hPa for latitudes between 20°S and 40°N (J. B. Kumer 1994, personal communication). The CLAES nitrous oxide climatology is derived from the Stratospheric and Mesospheric Sounder (SAMS) dataset merged with results from a two-dimensional model (see Kumer et al. 1993). The precision of nitrous oxide individual profiles (i.e., in an along-track view) at 46 hPa is about 20 ppbv (parts per billion by volume), and the accuracy is about 20%. The precision of nitrous oxide individual profiles at 4.6 hPa is 7 ppbv, and the accuracy is 20% (A. E. Roche 1994, personal communication).

Owing to the geometry of the *UARS* orbit (Reber 1993), *UARS* yaws through 180° at periods of approximately 35 days. This leads to an interval in which MLS and CLAES, which are limb viewers and thus sample the earth's atmosphere at right angles to the *UARS* orbit, sample latitudes from around 80°S to around 34°N, followed by an interval in which they sample latitudes from around 34°S to around 80°N. Because of this yaw maneuver data are unavailable for the high-latitude Northern Hemisphere for the periods 3 November–3 December 1991, 14 January–14 February 1992, 23 March–1 May 1992, and 1 June–12 July 1992. During the period 13–16 July 1992, when *UARS* was looking north, the MLS instrument was switched off, and no MLS data are available. At present there are no CLAES nitrous oxide data available prior to 9 January 1992.

The meteorological analyses used in this study are produced at the UKMO by the method of data assimilation. The observational data are primarily surface measurements, radiosonde profiles of wind and temperature, and atmospheric thicknesses derived from soundings made by operational weather satellites (Swinbank and O'Neill 1994). The version of the data used here does not include *UARS* measurements. The model used for the assimilation is a troposphere–stratosphere configuration of the UKMO Unified Model. The model uses a regular latitude–longitude grid of 2.5° × 3.75° and a hybrid vertical coordinate, which is terrain following near the ground, gradually becoming isobaric higher up. Currently, there are 42 vertical levels from the ground to 0.28 hPa, with a spacing in the stratosphere of approximately 1.6 km. The data used here are from the central archive, where the data are stored on pressure surfaces with six surfaces for each decade change in pressure.

The net diabatic heating rates are calculated using a radiative transfer algorithm provided by Haigh (1984). As input, MLS fields of water vapor, ozone, and temperature are used. Sensitivity tests in which these fields are perturbed by typical measurement uncertainties imply that calculated diabatic heating rates have a precision that is better than 10% in the stratosphere. In the tropical lower stratosphere, where net diabatic heating rates are small, calculated heating rates can differ in sign from rates calculated using other data and/or methods (see discussion in section 3).

Since consecutive *UARS* orbits differ by approximately 20° in longitude, gridding the data to produce

estimates of synoptic fields incurs a loss of horizontal detail. This is particularly true in the Northern Hemisphere where the circulation is highly nonzonal. Figure 1 shows a gridded field of MLS water vapor on 11 January 1992. Interpolation over large east–west distances leads to a distribution that is much more zonal than we would infer from meteorology and calculations of air-parcel trajectories. Moreover, the east–west interpolation smears out north–south structure evident along the viewing track of MLS. This difficulty is avoided by our use of viewing-track data. The MLS water vapor measurements are interpolated onto potential temperature θ surfaces in the stratosphere (465–1450 K, i.e., heights from approximately 20 to 42 km). The vertical interpolation is done along the MLS viewing track and uses MLS temperatures.

Although the MLS and CLAES measurements sample the same volume of the atmosphere, the CLAES orbit track exhibits data gaps. To overcome this, the MLS temperatures are gridded onto a regular latitude–longitude field and then interpolated onto the CLAES viewing track, after which the CLAES data are interpolated in the vertical onto potential temperature surfaces using MLS temperatures.

The chemical tracer fields along the viewing track are interpreted in the light of corresponding cross sections of wind speed, Ertel's potential vorticity (PV), and diabatic heating rates. Gridded fields of wind speed and PV derived from UKMO analyses are interpolated onto MLS viewing tracks on selected potential temperature surfaces using UKMO temperatures. Diabatic heating fields are treated in a similar way but using MLS temperatures in all computations.

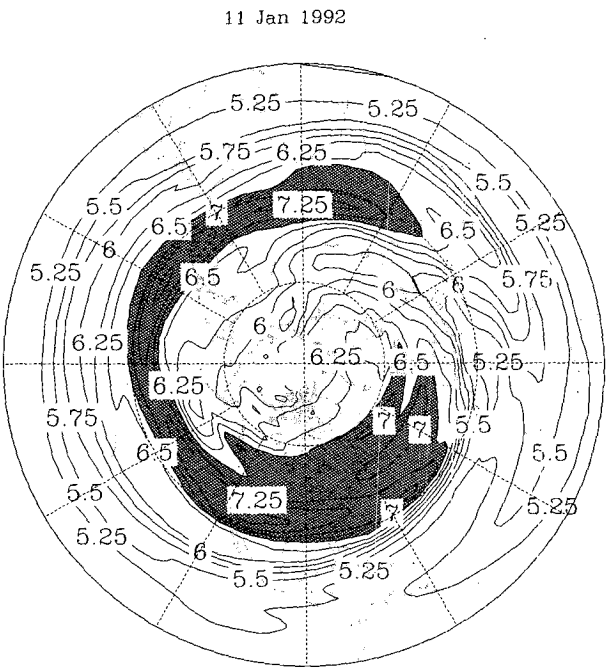

FIG. 1. Field of MLS water vapor mixing ratio (ppmv) at 1100 K (~35 km) for 11 January 1992 (*UARS* day 122). The map is on a polar stereographic projection from the equator to 90°N. The Greenwich meridian is located at three o'clock. The international date line is located at nine o'clock. The data were obtained by treating separately ascending and descending portions of the *UARS* orbit and then averaging. The contour step is 0.25 ppmv. The heavily shaded area is where water vapor mixing ratios exceed 6.75 ppmv.

3. Evolution of MLS water vapor in the Northern Hemisphere during 1991/92

In this section, we examine and interpret the seasonal evolution of MLS water vapor in the Northern Hemisphere from October 1991 to July 1992. The discussion is based on vertical cross sections of the mixing ratio taken along viewing tracks of the MLS instrument. These tracks are chosen to intersect the stratospheric polar vortex and the Aleutian high, as close as possible to the centers of the two vortices. The cross sections show several features of the water vapor distribution that evolve systematically. This evolution will be interpreted in the light of the large-scale stratospheric circulation. Concentrations of CLAES nitrous oxide will be used to corroborate features of transport inferred from the water vapor data.

a. Early winter 1991

1) OCTOBER 1991

(i) *Meteorology*

By October 1991, the stratospheric polar vortex was well developed in the Northern Hemisphere. The field of geopotential height at 10 hPa in Fig. 2 shows that the vortex lay almost symmetrically over the pole. A weak anticyclone, the Aleutian high, lay over the date line and was confined to the lower and middle stratosphere. Superimposed on the field is a viewing track of the MLS instrument that was chosen to cut the polar vortex and the Aleutian high approximately perpendicular to the jet stream that lies between them. The arrow shows the direction of motion along the track (further details of the track are given in the figure caption). This and similar cross sections (which correspond to single sweeps of the spacecraft orbit) extend across the polar cap from equator to equator and are chosen such that the Aleutian high is located on the left-hand side of the figure.

The distribution of wind speed along this viewing track is shown in Fig. 3. In this and similar wind speed cross sections solid isopleths denote flow into the plane of the cross section (into the page), and dashed isopleths denote flow out of the plane of the cross section (out of the page). Near the center of the figure, the pair of jet streams located on both sides of the pole at 60°N are the westerly jets associated with the polar vortex, which extends through the stratosphere. Its center is marked by the zero-wind line at 80°N. The easterly winds near 40°N to the left of the figure denote the

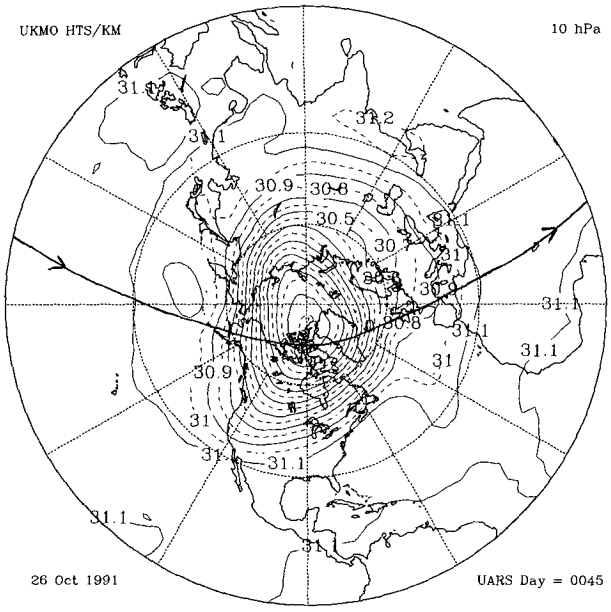

FIG. 2. Field of geopotential height (km) at 10 hPa from UKMO analyses for 26 October 1991 (*UARS* day 45). The contour step is 0.1 km. The map is on a polar stereographic projection from the equator to 90°N. The Greenwich meridian is located at three o'clock. The international date line is located at nine o'clock. Latitude circles are marked every 30°. Meridians are marked every 30°. Superimposed on the field is the viewing track of the MLS instrument, which refers to the cross section shown in Figs. 3 and 4. The arrow shows the direction of motion along the track.

equatorward flank of the Aleutian high. The associated closed anticyclonic circulation (flow out of the page at 60°N, flow into the page at 40°N) extends only up to about 40 km. Superimposed on the cross section is the 6-ppmv water vapor isopleth extracted from Fig. 4 (see below).

(ii) *Tracer cross sections*

A cross section of MLS water vapor mixing ratio along the viewing track marked in Fig. 2 is shown in Fig. 4. This field has potential temperature θ as the vertical coordinate, and the corresponding height values for a reference atmosphere are provided on the right-hand side of the figure. The vertical extent of the cross section is from about 20 to 2 hPa.

Generally speaking there is a strong vertical stratification in the water vapor mixing ratio, with values ranging from about 4 ppmv in the lower stratosphere to about 8 ppmv in the upper stratosphere. Isopleths over most of the domain in Fig. 4 dip down (with respect to reference values at low latitudes) each isopleth reaching its lowest altitude near the center of the polar vortex at *C*. The two notable exceptions are the regions *AB* and *DE*, where isopleths tend to bow upwards.

In the Tropics in the lower stratosphere, the relatively low mixing ratios of water vapor are consistent with the injection of freeze-dried air through the cold tropical tropopause (Brewer 1949; Dobson 1956). In the upper stratosphere and at high latitudes, the relatively high mixing ratios of water vapor are consistent with methane oxidation in the air rising in the upward extension of the Hadley circulation (Jones et al. 1986). The higher mixing ratio values therefore indicate a longer exposure of methane to the oxidation process.

The isopleths of water vapor mixing ratio dip down markedly within the polar vortex in the region *BCD*. For instance, the isopleth marked in bold (which represents a mixing ratio of 6 ppmv) drops by up to 10 km from the periphery of the polar vortex to is center. The tracer distribution in the region *BCD* is roughly axisymmetric about an axis coincident with the center of the vortex (at *C*), showing that the polar vortex strongly organizes the distribution of tracers in its vicinity.

In the jet streams at *B* and *D* horizontal gradients of mixing ratio decrease rapidly toward the center of the vortex; this arrangement persists until February. In the Aleutian high (between *A* and *B*), and to some extent in the southern flank of the jet stream between *D* and *E*, gradients change sign rapidly. At *A* lies another band of strong horizontal gradients in the westerly jet stream to the south of the Aleutian high. This region of strong gradients has a counterpart at *E* on the opposite side of the polar vortex. We will argue that the high gradients noted in Fig. 4 are caused by a combination of descent through the isentropic surfaces due to radiative cooling and lateral advection in and around the polar vortex and the Aleutian high.

2) DECEMBER 1991: DESCENT OF TRACER ISOPLETHS

In December 1991 (Fig. 5) the MLS water vapor shows the same structure as in late October (Fig. 4), namely, strong isentropic gradients at midlatitudes (marked *B* and *D*) and at low latitudes (marked *A* and *E*). The notable difference is that the 6-ppmv isopleth and others nearby have descended in 45 days by 2–3 km, or by 150 K (in potential temperature), inside the vortex (the region marked *BCD*). Isentropic gradients imply that this descent of the isopleths cannot be the result of isentropic advection but must have arisen by descent of moister air through isentropic surfaces. On this basis, we estimate a cooling rate in the midstratosphere in early winter of about 1 K in temperature per day. Direct calculation of the cooling rate using the radiative transfer algorithm of Haigh (1984) gives descent rates of about 1–2 K day^{-1} in the midstratosphere within the vortex.

b. Midwinter 1991/92

1) JANUARY 1992

(i) *Meteorology*

By January 1992 the polar vortex was well developed throughout the stratosphere of the Northern Hemi-

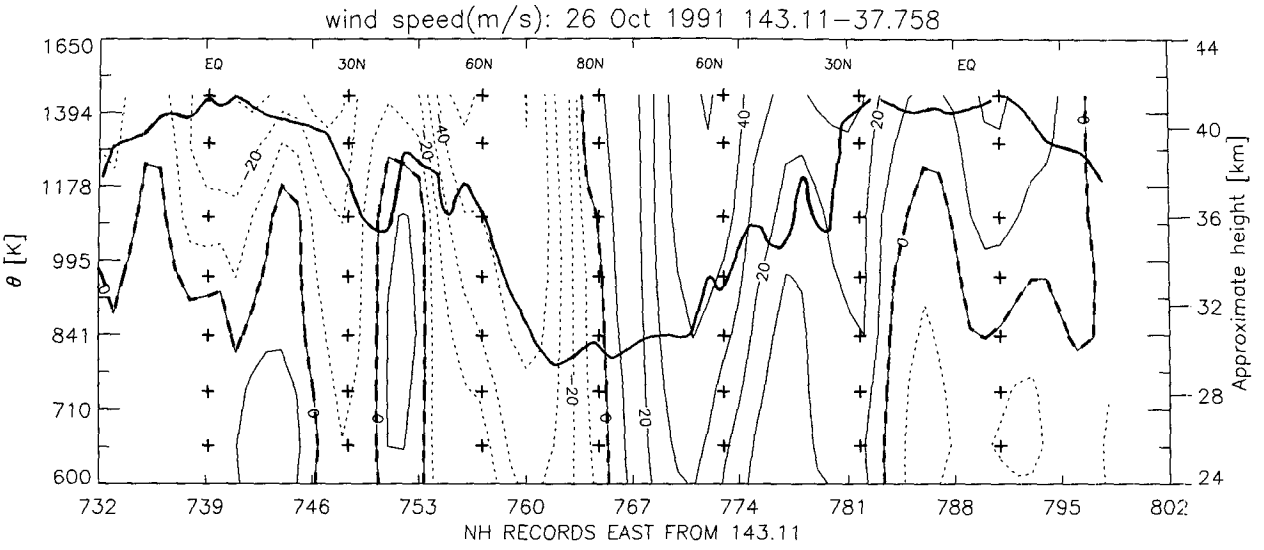

FIG. 3. Record number versus θ (K) cross section of UKMO-analyzed wind speeds (m s^{-1}) along the viewing track shown in Fig. 3 for 26 October 1991 (*UARS* day 45). The track goes from about 20°S, 143°E to 20°S, 38°E. The abscissa indicates the record number associated with the MLS water vapor measurement. [There are 1318 or 1319 MLS records, i.e., MLS profile measurements, in one day. Greenwich mean time (in hours) of the record number is record number times 24 divided by the records in one day]. The ordinate indicates potential temperature. Marked on the right-hand side of the figure are the corresponding height values for a reference atmosphere. The location of the equator, 30°, 60°, and 80°N latitude circles along the viewing track is marked at the top of the figure by the crosses. The position of the crosses indicates the potential temperature levels θ to which the wind speeds have been interpolated. The zero-wind line is marked by the thick dashed line. The contour step is 10 m s^{-1}. Dashed lines indicate motion out of the page, and solid lines indicate motion into the page. Superimposed on the field (thick solid line) is the 6-ppmv water vapor isopleth associated with the viewing track of the MLS instrument shown in Fig. 4. The local solar times are, in ascending record number along the abscissa, approximately 1.3 h (30°N), 7.8 h (80°N), 14.6 h (30°N).

sphere (O'Neill et al. 1994). The field of geopotential height at 10 hPa in Fig. 6 shows that the vortex was shifted off the pole and the Aleutian high was well developed. Superimposed on the field is a viewing track of the MLS instrument (details of the track are given in the caption).

The distribution of wind speed along this viewing track is shown in Fig. 7. The strong polar vortex is centered near 70°N (at the zero-wind line to the right of center of the figure). The Aleutian high is now a much stronger feature of the circulation and extends right through the stratosphere as evidenced by the vertical extent of the easterlies between 30° and 60°N (on the left of the figure), which are associated with the closed anticyclonic circulation centered at the zero-wind line near 60°N. Superimposed on the cross section is the 6-ppmv water vapor isopleth extracted from Fig. 8 (see below).

(ii) *Tracer cross sections*

Figure 8 typifies the distribution of water vapor across the polar vortex and Aleutian high in midwinter. As above it helps to refer the 6-ppmv isopleth to the cross section of wind speed as in Fig. 7. In the polar vortex (marked *BCD*) the isopleths of water vapor mixing ratio dip sharply downward by up to about 15 km from the periphery of the vortex to its center (at *C*) (because the viewing track does not quite go through the center of the vortex the zero-wind line and the point of maximum descent of the 6-ppmv isopleth do not coincide). Associated with this dip in the isopleths, water vapor concentrations increase sharply across the jet streams (*B* and *D*) toward the center of the vortex. In the Aleutian high, however, horizontal gradients are, characteristically, not monotonic but change sign over short distances, so that on average, isentropic gradients are much weaker in the Aleutian high than they are in the polar vortex. This contrast between the polar vortex and the Aleutian high is explained below.

On the southern flank of the polar vortex, diametrically opposite the Aleutian high, is a "ridge" of relatively dry air (at *D* in Fig. 8). This ridge extends over 12 km in the vertical and is associated with the eastward advection, around the polar vortex, of a narrow streamer of relatively dry air from low latitudes. Its location coincides exactly with a streamer of air distinguished by high values of nitrous oxide, as shown by the cross section in Fig. 9 at the point marked *D*. Similar features have been found in fields of nitrous oxide derived from the Improved Stratospheric and Mesospheric Sounder (ISAMS) on *UARS* (Ruth et al. 1994). The ridge in water vapor also coincides with a distinct local minimum in PV at the point marked *D* in Fig. 10. Synoptic maps of PV and calculation of air parcel trajectories (O'Neill et al. 1994) confirm that

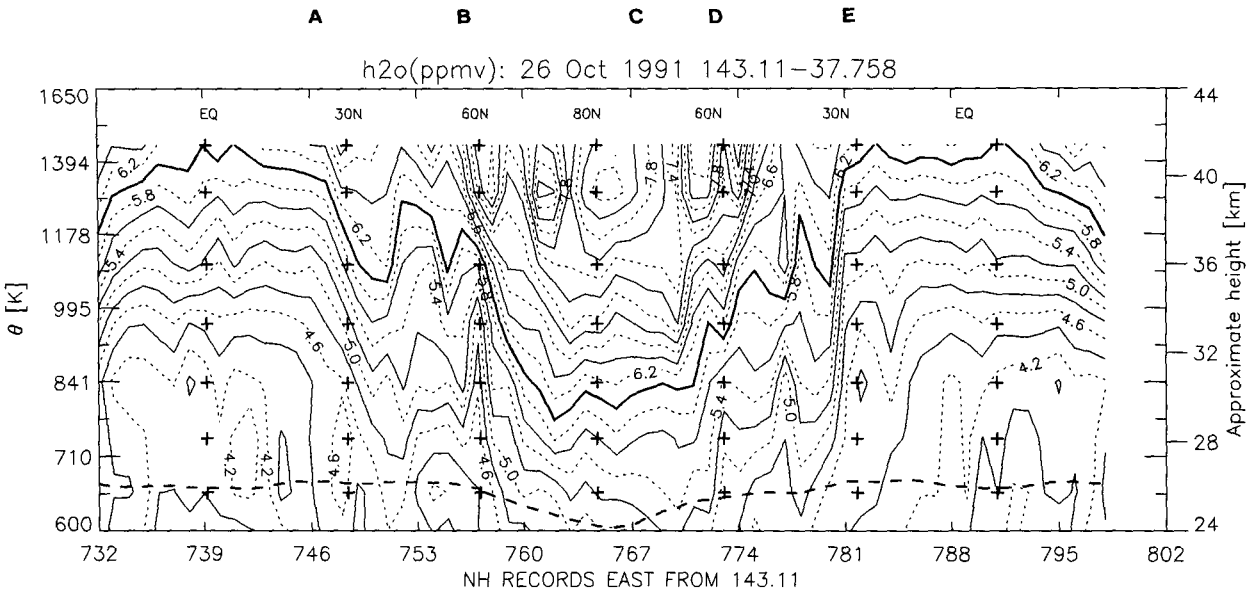

FIG. 4. As Fig. 3 but for MLS water vapor (ppmv) data on 26 October 1991 (*UARS* day 45) along the viewing track shown in Fig. 2. The 6-ppmv isopleth is marked in bold. The contour step is 0.2 ppmv. The θ level at which the pressure is 22 hPa is marked by the bold dashed line.

these localized features of the tracer fields arise by quasi-horizontal eastward advection of air around the polar vortex on an isentropic surface. Trajectories show further that the streamer of relatively dry air is subsequently advected along the jet stream between the polar vortex and the Aleutian high, which accounts for the ridge of relatively dry air in Fig. 8 near *B*.

The trajectory calculations of O'Neill et al. (1994) indicate that the streamer of air ultimately spirals into the anticyclonic circulation associated with the Aleutian high. Evidence for this spiraling of material in the Aleutian high is provided by the series of local minima in water vapor mixing ratio interspersed between local maxima across the region of closed anticyclonic cir-

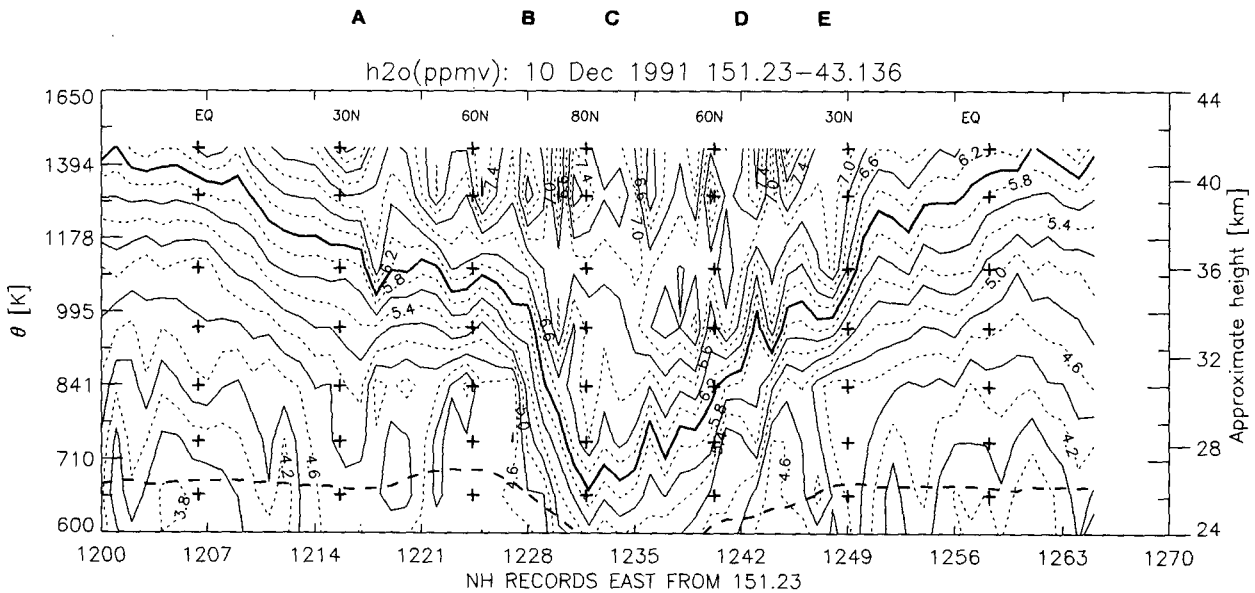

FIG. 5. As Fig. 4 but for MLS water vapor (ppmv) data on 10 December 1991 (*UARS* day 90). The viewing track goes from about 20°S, 151°E to 20°S, 43°E. The local solar times are, in ascending record number along the abscissa, approximately 10.2 h (30°N), 16.4 h (80°N), 23.5 h (30°N).

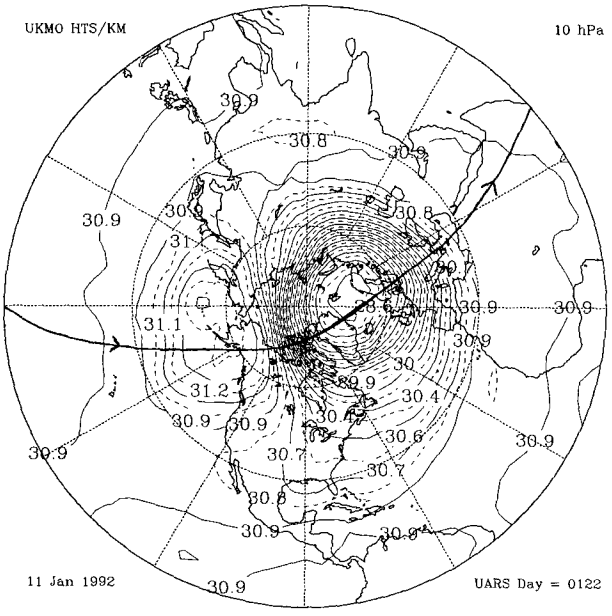

FIG. 6. As Fig. 2 but for the geopotential height field (km) at 10 hPa from UKMO analyses for 11 January 1992 (*UARS* day 122). Superimposed on the field is the viewing track of the MLS instrument, which refers to Figs. 7–11. The arrow shows the direction of motion along the track.

culation, marked *AB* in Fig. 8. The features have counterparts in the cross section of nitrous oxide (Fig. 9), although they do not coincide exactly. This spiraling of air with a given mixing ratio into the Aleutian high, where the circuit time is a few days, accounts for our earlier observation that gradients of mixing ratio change sign several times in the Aleutian high but are, on average, weak compared with gradients in the polar vortex.

The contrast in the tracer gradients in the two vortices attests to significant differences in the advection of material lines. The persistence of strong horizontal gradients in the jet stream around the polar vortex signifies that material lines are aligned with flow lines. Stretching and folding of material lines in the jet is suppressed by the strong horizontal gradients of PV (the Rossby wave restoring mechanism). In fact, radial gradients increase with time until late winter as a result of diabatic cooling and descent of air through isentropic surfaces. By contrast, there is now ample evidence that in the Aleutian high material lines are coiled up [as originally suggested by McIntyre and Palmer (1983)], so that air masses with different properties are mixed down to scales well below the resolution of instruments such as MLS (see Fig. 11 in O'Neill et al. 1994). Hence, radial gradients are weak in the Aleutian high (apart from small-scale structure).

(iii) *Descent of tracer isopleths*

Figure 11 typifies the distribution of calculated diabatic heating rates across the polar vortex and the Aleutian high in midwinter. In the upper-stratosphere Tropics there is ascent, (heating) and elsewhere in the Northern Hemisphere there is descent (cooling). The strongest cooling is around 70°N, in the strong baro-

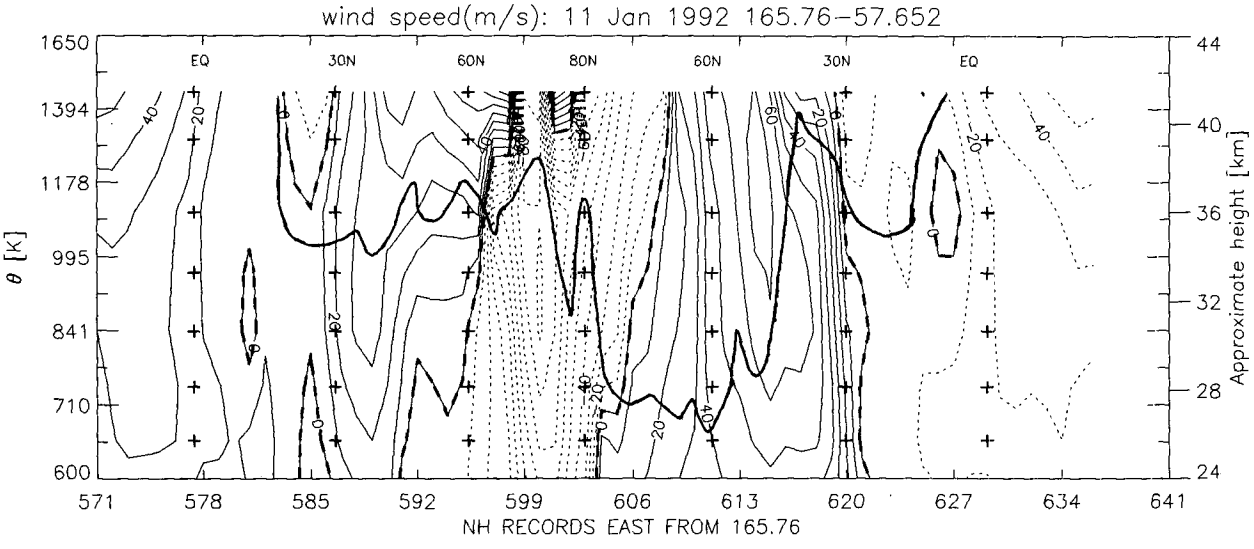

FIG. 7. As Fig. 3 but for UKMO-analyzed wind speeds (m s^{-1}) on 11 January 1992 (*UARS* day 122) along the viewing track, which is shown in Fig. 6. The contour step is 10 m s^{-1}. Dashed lines indicate motion out of the page, and solid lines indicate motion into the page. Superimposed on the wind speed field is the 6-ppmv water vapor isopleth associated with the cross section shown in Fig. 8. The track is from about 20°S, 141°E to 20°S, 33°E. The local solar times are, in ascending record number along the abscissa, approximately 23.8 h (30°N), 6 h (80°N), 13 h (30°N).

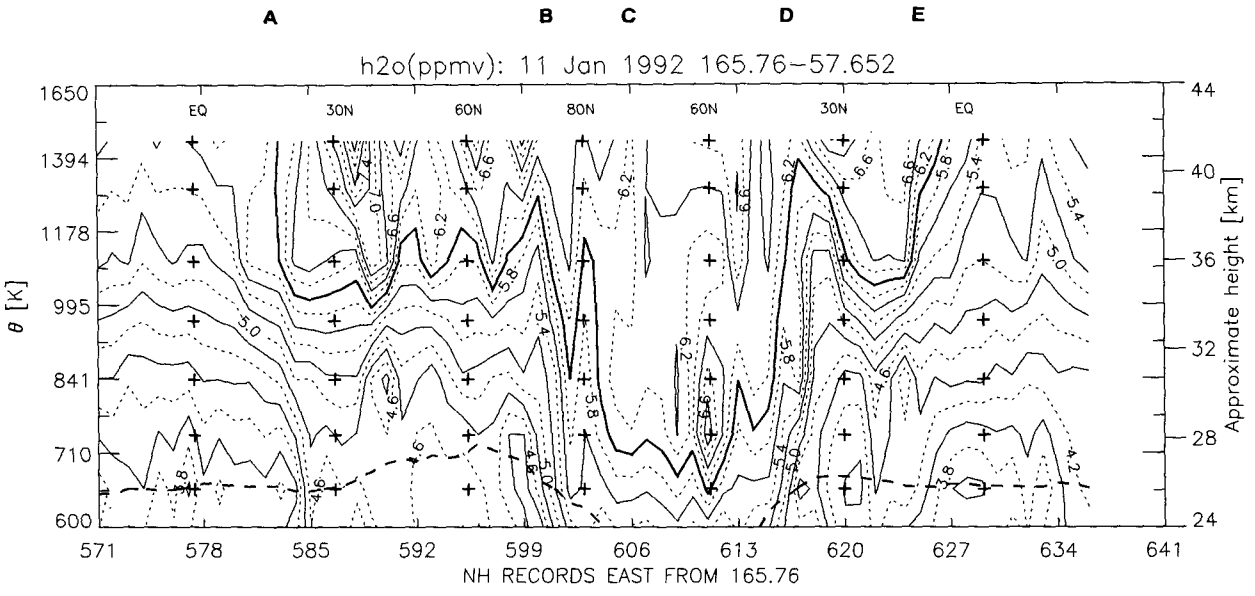

FIG. 8. As Fig. 4 but for MLS water vapor (ppmv) data on 11 January 1992 (*UARS* day 122) along the viewing track shown in Fig. 8.

clinic region between the polar vortex and the Aleutian high (located near *B*). There is also strong cooling around 60°N near *D* due to the presence of a developing anticyclone that is traveling eastward around the polar vortex (O'Neill et al. 1994). Note that the calculation for January (as well as for February—see Fig. 14) gives small negative diabatic heating rates in the lower-stratosphere Tropics, where one would expect small positive values (see, e.g., Olaguer et al. 1992). This indicates inadequacies in the input data and/or the method for this region. In the regions of the stratosphere germane to the discussion in this paper, the net diabatic heating rates agree qualitatively with the results of Olaguer et al. (1992).

The sharp gradients in the water vapor cross section at *A* and *E* are due to a tilting of the water vapor isopleths from the horizontal to the vertical as a consequence of ascent in the upper-stratosphere Tropics and descent in the midlatitude upper stratosphere. Trajectory calculations of Sutton et al. (1994) indicate that

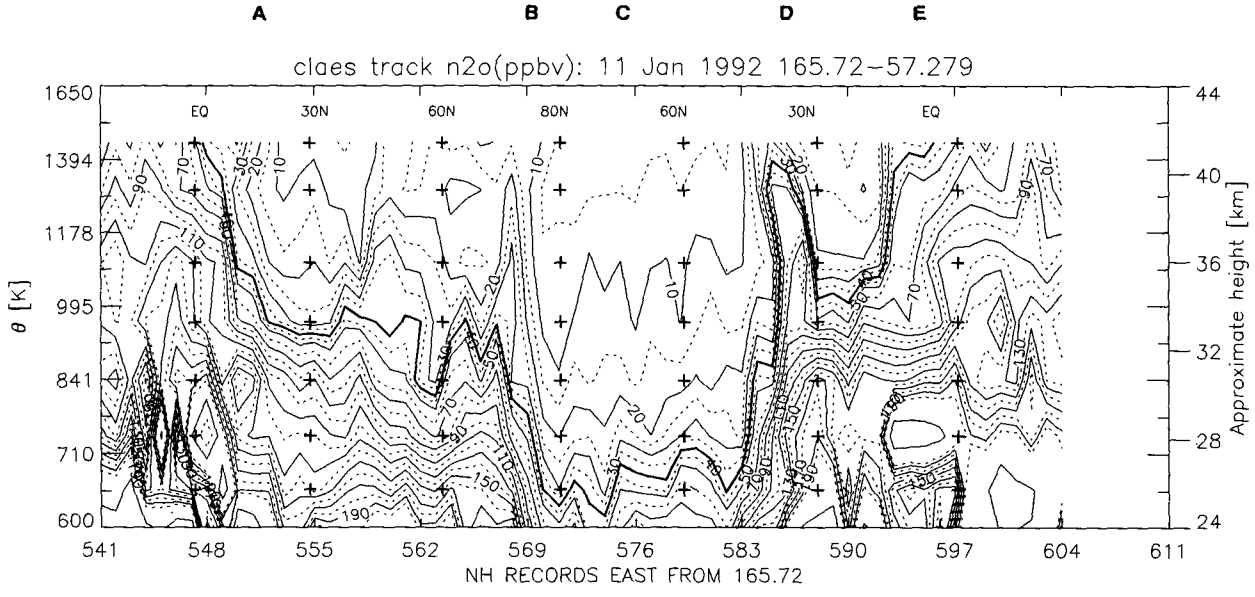

FIG. 9. As Fig. 8 but for CLAES nitrous oxide (ppbv) data on 11 January 1992 (*UARS* day 122). The 40-ppbv isopleth is marked in bold. The contour step is 10 ppbv for mixing ratios greater than 50 ppbv and 5 ppbv for mixing ratios less than 50 ppbv.

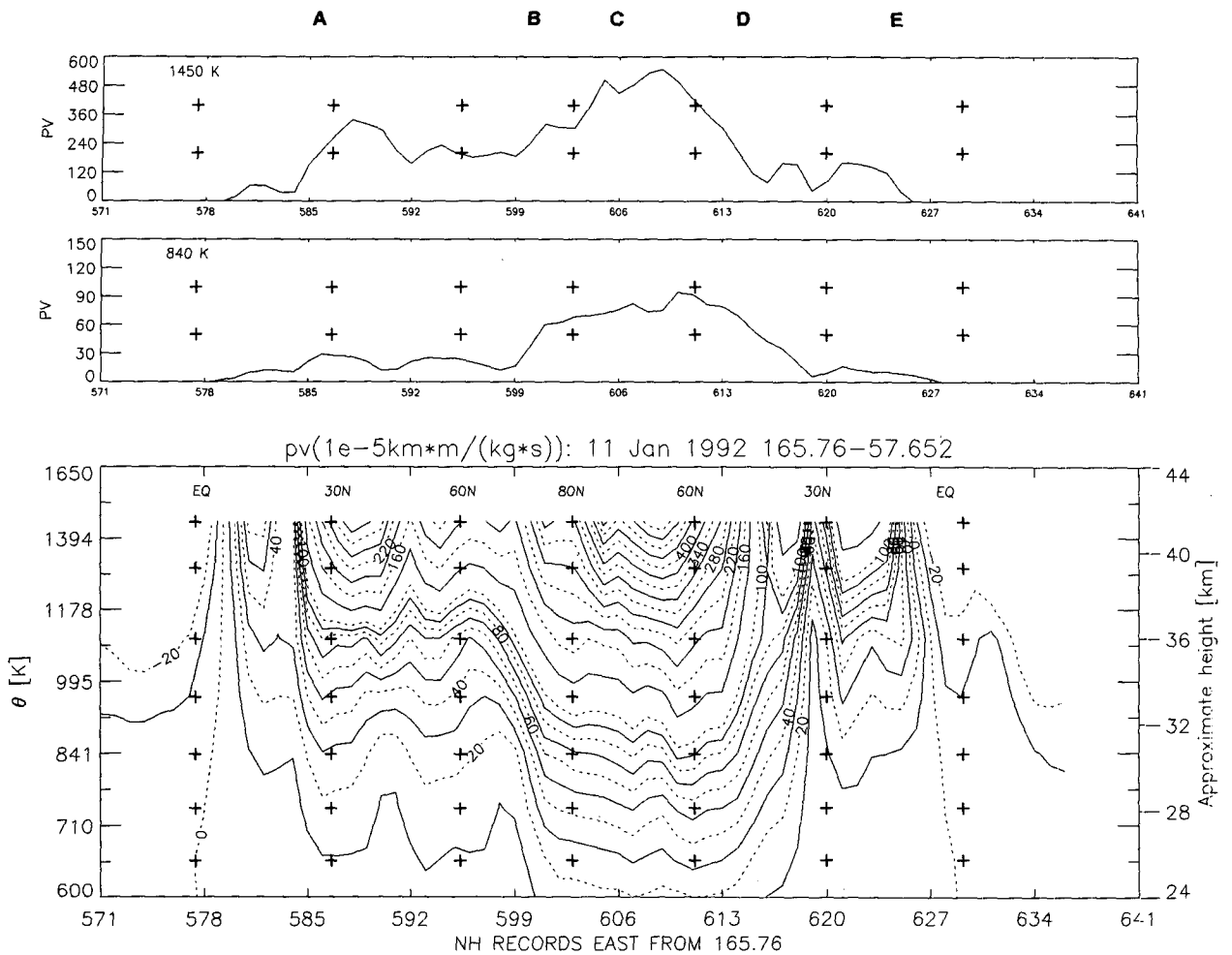

FIG. 10. Bottom panel: as Fig. 8 but for UKMO-derived isentropic PV (PV units; 1 PV unit = 10^{-5} K m^2 kg^{-1} s^{-1}). The contour step is 10 PV units for values less than 100 PV units and 30 PV units for values greater than 100 PV units. Middle panel: UKMO-derived isentropic PV cut at 840 K (~30 km) along the cross section shown in the bottom panel of Fig. 10. Top panel: UKMO-derived isentropic PV cut at 1450 K (~42 km) along the cross section shown in the bottom panel of Fig. 10. The middle and top panels have crosses to mark the location of the equator, 30°, 60°, and 80°N latitude circles.

eastward advection, around the vortex, of low-latitude air that is then fed into the anticyclonic circulation of the Aleutian high also contributes toward sharpening the gradients at *A*. The location of these gradients coincides exactly with high gradients in the nitrous oxide distribution, as shown by the cross section in Fig. 9 at the points marked *A* and *E*, and with high gradients in the PV distribution at the points marked *A* and *E* in Fig. 10.

Recent high-resolution trajectory studies of the northern winter stratosphere (V. Pope 1994, personal communication) suggest that the strongest descent (in an average sense) is located in the Aleutian high and in a ring inside the polar vortex. Given the organization of the large-scale flow by the polar vortex and the Aleutian high, this pattern of descent would lead to filamentary curtains of material extending throughout the depth of the anticyclone and a double peak in the tracer distribution inside the polar vortex.

Neither the filamentary curtains of material nor the double peak in the polar vortex is observed in the MLS water vapor or the CLAES nitrous oxide cross sections, where the isopleths dip strongly from the periphery of the vortex to the center of the vortex (see Figs. 8 and 9). The fact that filamentary curtains of material in the anticyclone are lacking in the observations is due to the coarse resolution of the satellite data. The fact that a double peak in the polar vortex is lacking in the observations could be due to the coarse resolution of the satellite data and/or to stretching and folding that has taken place at the bottom of the polar vortex and that is not captured in high-resolution trajectory models.

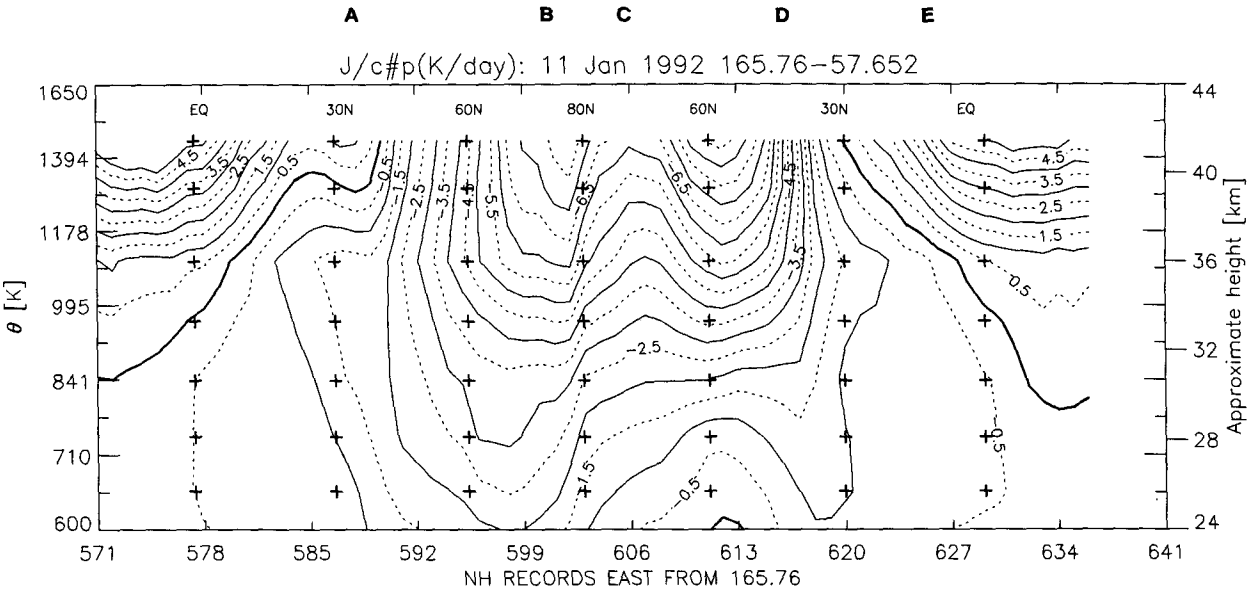

FIG. 11. As Fig. 8 but for calculated net diabatic heating rate (K day^{-1}). The zero heating isopleth is marked in bold. The contour step is 0.5 K day^{-1}.

2) FEBRUARY 1992: RELATIVE DRYNESS OF STRATOSPHERIC AIR

Figure 12 typifies the distribution of water vapor across the polar vortex and Aleutian high in mid-February 1992. In the polar vortex (marked *BCD*, with *C* its center) the water vapor isopleths of mixing ratio have been lifted by about 4 km with respect to their location in mid-January (see Fig. 8). The horizontal gradients of water vapor mixing ratio in this region are now, characteristically, not monotonic but change sign over short distances so that, on average, isentropic gradients in the polar vortex are much weaker in mid-February than in mid-January. By contrast, Fig. 13 shows that, in the polar vortex, the nitrous oxide isopleths of mixing ratio have remained roughly at the same isentropic level as in mid-January (see Fig. 9). Other features that were observed in mid-January, for example, the high quasi-horizontal gradients at low latitudes, are also present in mid-February (marked *A* and *E* in Figs. 12 and 13).

The persistence of the relative dryness of the midstratosphere polar vortex throughout the period from mid-February to mid-March suggests that it is real. The observed distribution of water vapor in the middle atmosphere (Bevilacqua et al. 1983; Jones et al. 1986; Harwood et al. 1993) indicates that possible sources of the relatively dry air mass observed in mid-February are (a) the lower stratosphere, (b) midlatitudes and/or the Tropics, and (c) the mesosphere for heights greater than about 65 km.

The observed distributions of nitrous oxide in the middle atmosphere (Gunson et al. 1990; Kumer et al. 1993) indicate that nitrous oxide values generally decrease with increasing height and with increasing poleward displacement from the tropics. This rules out ascent from the lower stratosphere as a mechanism for drying the midstratosphere, as it would bring nitrous oxide-rich air to midstratospheric levels and lift the nitrous oxide isopleths in mid-February with respect to their location in mid-January, in contradiction to what is observed (compare Figs. 9 and 13). Calculation of cooling rates gives descent rates of around 1–2 K day^{-1} in the midstratosphere polar vortex in the period from mid-February to mid-March (see, e.g., Fig. 14). This also tends to rule out ascent of lower-stratospheric air as a mechanism for drying the midstratosphere.

The persistence of strong quasi-horizontal gradients in nitrous oxide mixing ratio in the jet stream around the polar vortex signifies that material lines are aligned with flow lines. The presence of similar strong quasi-horizontal gradients of PV (marked *B* and *D* in Fig. 15) indicates that stretching and folding is suppressed in the jet and that little or no large-scale transport across the jet stream is taking place. This tends to rule out large-scale quasi-horizontal transport from lower latitudes into the vortex as a mechanism for drying the midstratosphere.

Descent of relatively dry mesospheric air to the midstratosphere would advect downward nitrous oxide–poor air (Gunson et al. 1990), in agreement with the observed nitrous oxide cross section (see Fig. 13). The arrival of relatively dry mesospheric air in the midstratosphere at levels around 840 K in mid-February ought to have a signature as it passes through higher-stratospheric levels. This signature is observed in a consistent manner around the 1100-K level in the period

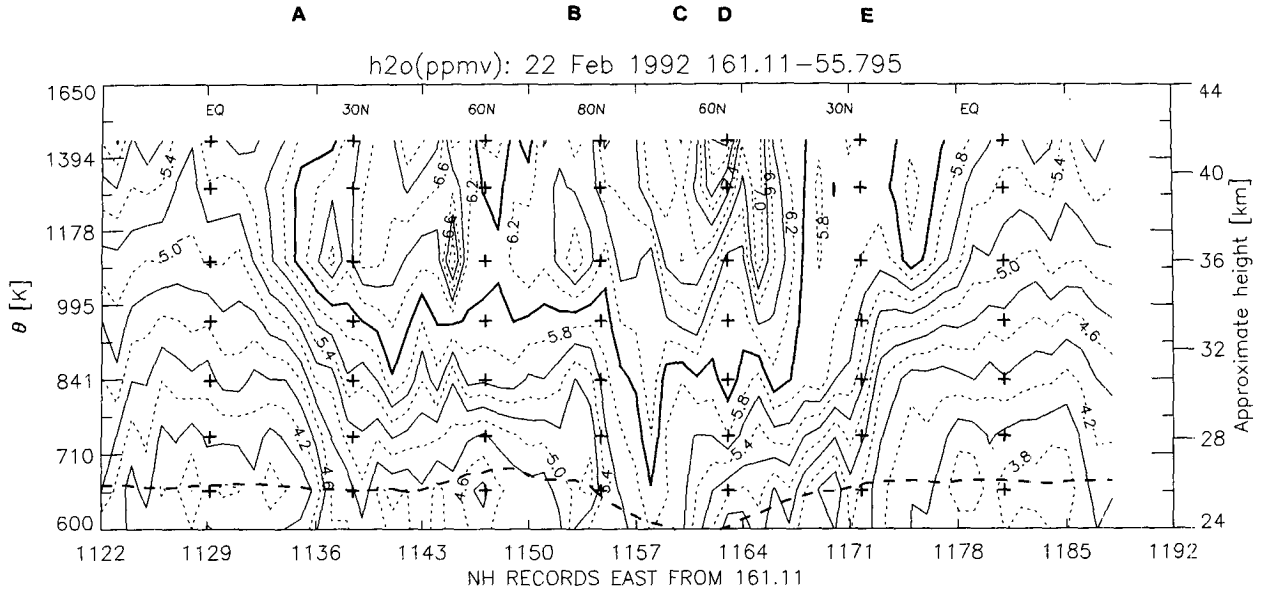

FIG. 12. As Fig. 8 but for MLS water vapor (units of ppmv) data on 22 February 1992 (*UARS* day 164). The viewing track is from about 20°S, 161°E to 20°S, 56°E. The local solar times are, in ascending record number along the abscissa, approximately 9.6 h (30°N), 16.1 h (80°N), 22.9 h (30°N).

from mid-December to mid-January (see, e.g., Fig. 8 around record number 610, where a local minimum in the water vapor profile is observed). This descent of air in the vortex of about 5 km, or 250 K (in potential temperature), in about a month allows us to estimate a cooling rate in the midstratosphere in midwinter of about 2.5 K day^{-1}. Direct calculation of the cooling rate using the radiative transfer algorithm of Haigh (1984) gives descent rates of about 2–3 K day^{-1} in the midstratosphere within the vortex.

Descent of mesospheric air to the midstratosphere has been predicted in the Southern Hemisphere using a global model (Fisher et al. 1993) and observed in satellite data in the Southern Hemisphere (Russell et al. 1993). Recent modeling studies (Sutton 1994) suggest that during the autumn and winter period air can

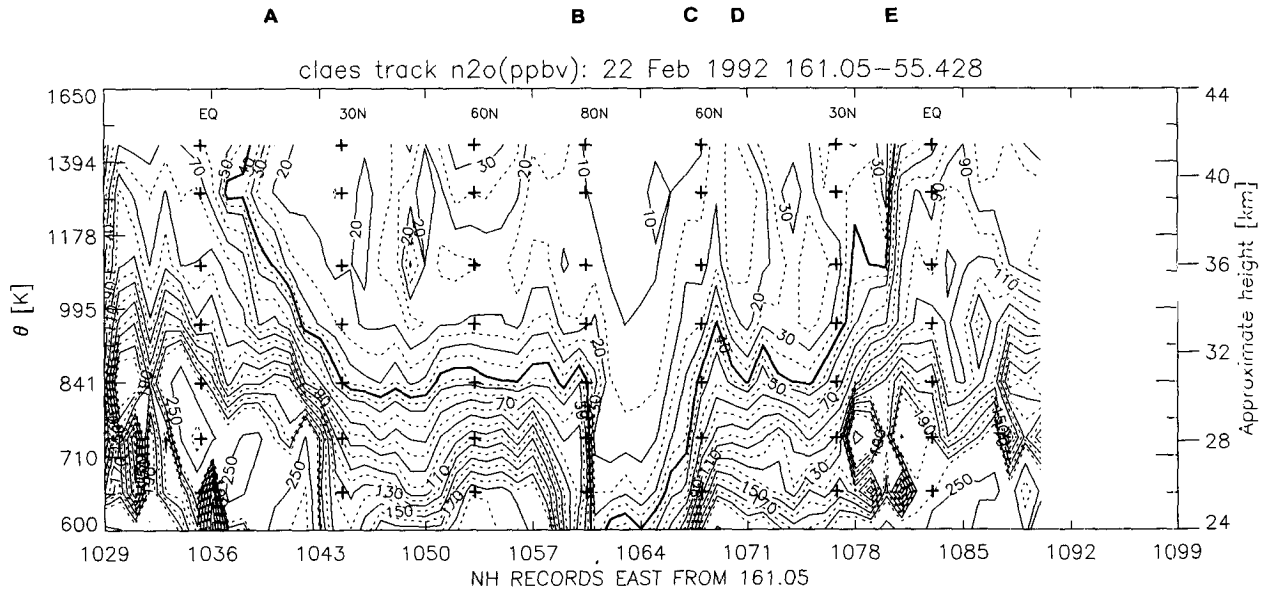

FIG. 13. As Fig. 12 but for CLAES nitrous oxide (ppbv) data on 22 February 1992 (*UARS* day 164).

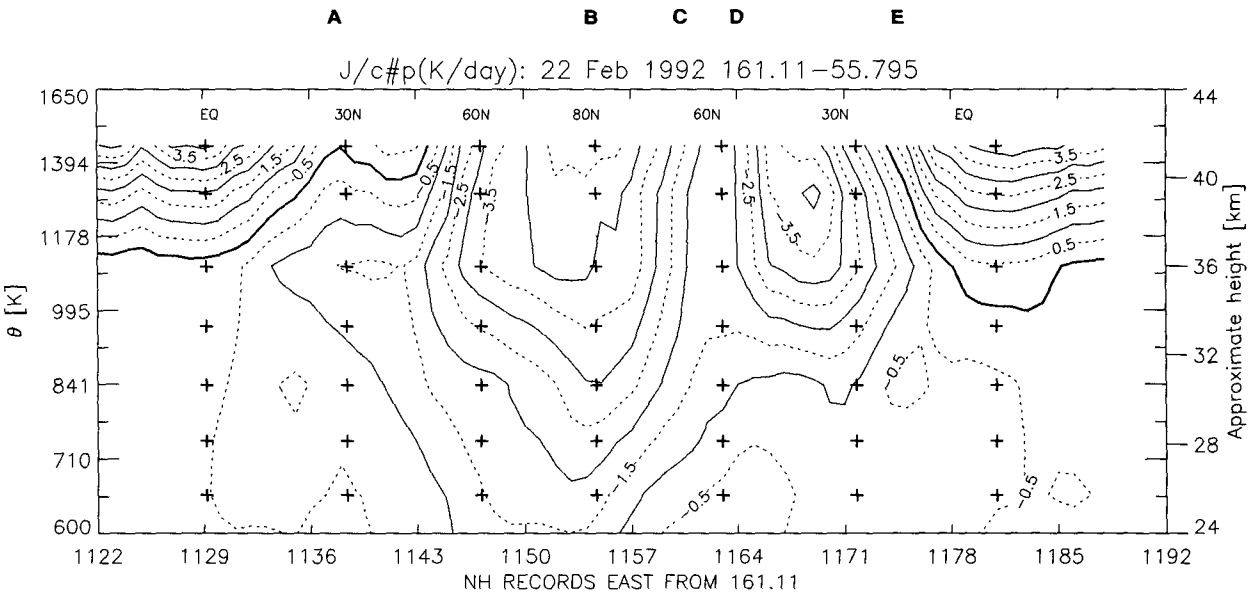

FIG. 14. As Fig. 12 but for calculated net diabatic heating rate (K day^{-1}).

descend in a coherent fashion from the mesosphere to the lower stratosphere over a time interval of about 4–5 months. The studies of Sutton (1994) also suggest that, starting from the beginning of autumn, and over a time interval of about 3 months, there is a "pipeline" connecting the mesosphere to the midstratosphere and that this pipeline may be severed after a time interval of about 4–5 months.

Such a pipeline is not observed in the water vapor cross sections or the nitrous oxide cross sections for January or February. This may be due to the coarse resolution of the satellite data and/or the possibility that the pipeline may have been severed. During the period 14 January–14 February 1992 (in which MLS and CLAES were looking south) there was a minor warming (O'Neill et al. 1994), which conceivably could have severed the pipeline connecting the mesosphere to the midstratosphere.

Of the three mechanisms proposed to explain the relative dryness observed in the midstratosphere—namely, (a) ascent from the lower stratosphere, (b) large-scale horizontal advection from lower latitudes into the polar vortex, and (c) descent of mesospheric air to the midstratosphere, only the latter is consistent with the observed cross sections of water vapor, nitrous oxide, PV, and diabatic heating. These viewing-track analyses, therefore, support the conclusions put forward by Lahoz et al. (1993), which stated that descent of relatively dry mesospheric air to the midstratosphere was taking place and that this descent dried the interior of the polar vortex.

The possibility of a mechanism different from the ones considered above that is responsible for the observed relative dryness in the midstratosphere cannot be ruled out. This is an issue that should be investigated using high-resolution trajectory studies and/or modeling studies.

c. *Late winter 1992*

1) MARCH 1992

(i) *Meteorology*

By the middle of March 1992 the stratospheric polar vortex was still relatively strong and the anticyclone had not developed to a strength comparable to that of the polar vortex. By late March (when MLS and CLAES were looking south) the polar vortex was small and weak and strongly distorted with an anticyclone of almost equal strength close to the pole. The evolution of the final warming during the spring of 1992 is typical of a strong dynamical final warming with a "top-down" breakdown of the vortex (O'Neill et al. 1994).

(ii) *Tracer cross sections*

In mid-March 1992 (Fig. 16) the MLS water vapor shows very similar structure to that observed in mid-February (Fig. 12), namely, strong isentropic gradients at low latitudes (marked *A* and *E*), and a lifting of the isopleths of mixing ratio in the polar vortex (marked *BCD*, with *C* its center) with respect to their location in mid-January (see Fig. 8). The CLAES nitrous oxide for mid-March (Fig. 17) also shows very similar structure to that observed in mid-February. The strong isentropic gradients at low latitudes (marked *A* and *E*) have been maintained, and in the polar vortex, the nitrous oxide isopleths of mixing ratio have remained

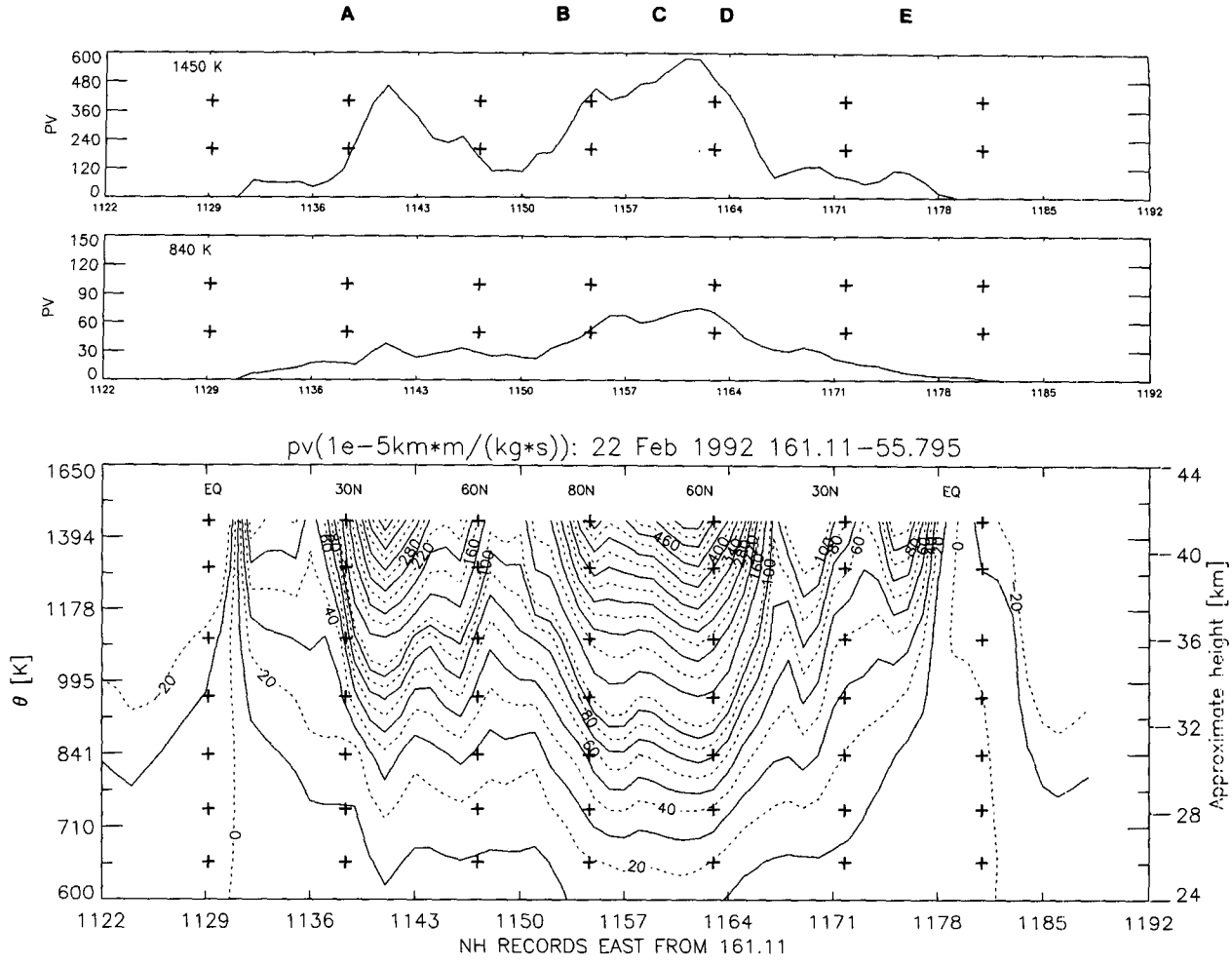

FIG. 15. Bottom panel: as Fig. 12 but for UKMO-derived isentropic PV (PV units; 1 PV unit = 10^{-5} K m^2 kg^{-1} s^{-1}). Middle panel: UKMO-derived isentropic PV cut at 840 K (~30 km) along the cross section shown in the bottom panel of Fig. 15. Top panel: UKMO-derived isentropic PV cut at 1450 K (~42 km) along the cross section shown in the bottom panel of Fig. 15.

roughly at the same level as in mid-January (see Fig. 9). Between mid-February and mid-March the water vapor and nitrous oxide isopleths in the midstratosphere polar vortex have remained roughly at the same level, possibly due to the relatively small cooling rates present at these stratospheric levels at this time of the year.

2) MAY–JULY 1992

(i) *Tracer cross sections*

In early May (Fig. 18) MLS water vapor shows relatively strong quasi-horizontal gradients at low latitudes (marked *A* and *E*). These gradients are less steep than in mid-March (see Fig. 16) due to the uniform and weak diabatic ascent that takes place throughout the Northern Hemisphere upper stratosphere. In the region poleward of 45°N quasi-horizontal gradients are, characteristically, not monotonic but change sign over short distances, so that, on average, isentropic gradients are weak in this region. The presence of these weak gradients is due to the breakup of the polar vortex, which has enabled midlatitude and high-latitude air masses to mix through stretching and folding of material lines.

(ii) *Descent of tracer isopleths*

In mid-July 1992 (Fig. 19) the MLS water vapor shows structure as in early May with two notable exceptions. First, the gradients at low latitudes in the Northern Hemisphere (marked *A* and *E*) have steepened in mid-July due to stronger diabatic ascent over the tropics. Direct calculation of the heating rate using the radiative transfer algorithm of Haigh (1984) gives ascent rates of about 1–4 K day^{-1} in early May, and of about 3–5 K day^{-1} in mid-July. Second, the water vapor cross section for mid-July shows relatively strong quasi-horizontal gradients at low latitudes in the

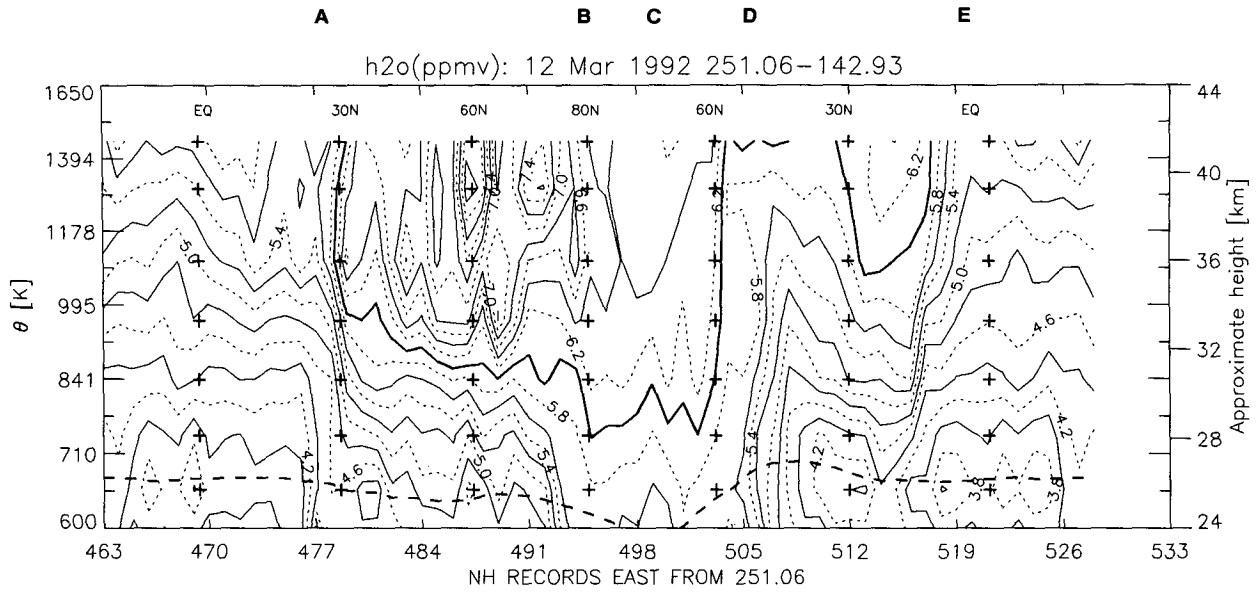

FIG. 16. As Fig. 4 but for MLS water vapor (ppmv) data on 12 March 1992 (*UARS* day 183). The viewing track is from about 20°S, 251°E to 20°S, 143°E. The local solar times are, in ascending record number along the abscissa, approximately 3.5 h (30°N), 9.7 h (80°N), 16.7 h (30°N).

Southern Hemisphere (marked *AS* and *ES*). These gradients are associated with the onset of southern winter and are analogous to the strong gradients at low latitudes observed in, for example, December 1991 (marked *A* and *E* in Fig. 5).

4. Conclusions

We have documented the northern winter stratosphere of 1991/92 by following the structure and evolution of MLS water vapor isopleths in a vortex-centered picture. This approach takes into account the general lack of axial symmetry in the northern winter stratosphere and avoids the misinterpretation of data that can arise from the traditional wave–mean flow interaction picture. By taking a viewing-track picture we have used the satellite data to its fullest potential and avoided the loss of detail associated with the gridding of satellite data. We have demonstrated that the water vapor distributions show clear signatures of the effects

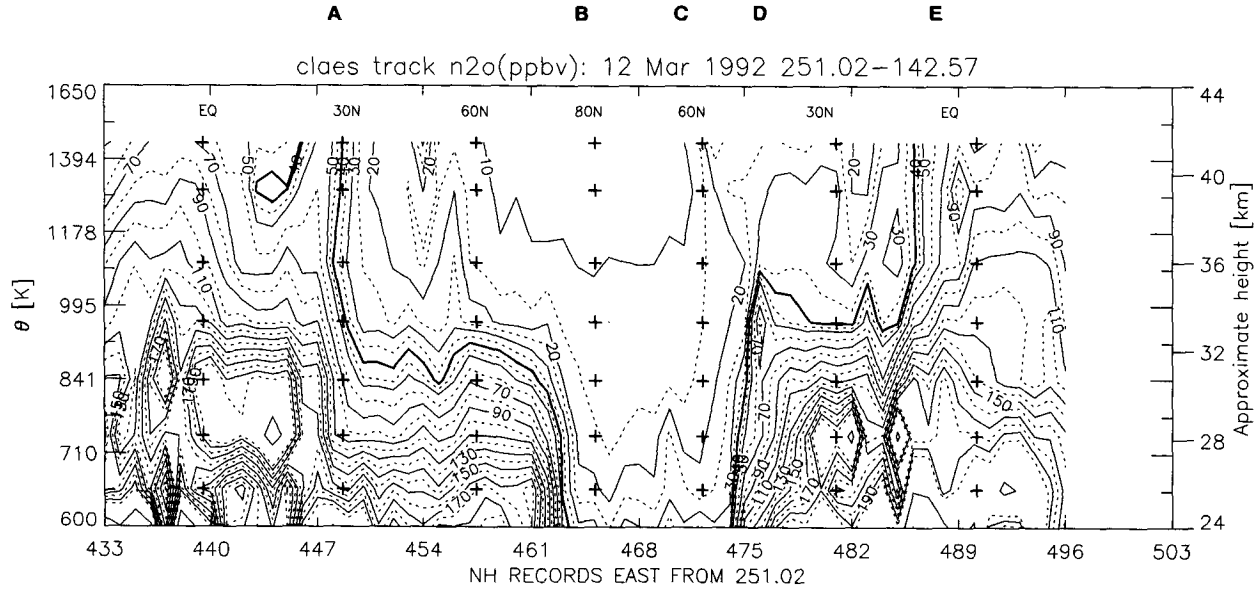

FIG. 17. As Fig. 16 but for CLAES nitrous oxide (ppbv) data on 12 March 1992 (*UARS* day 183).

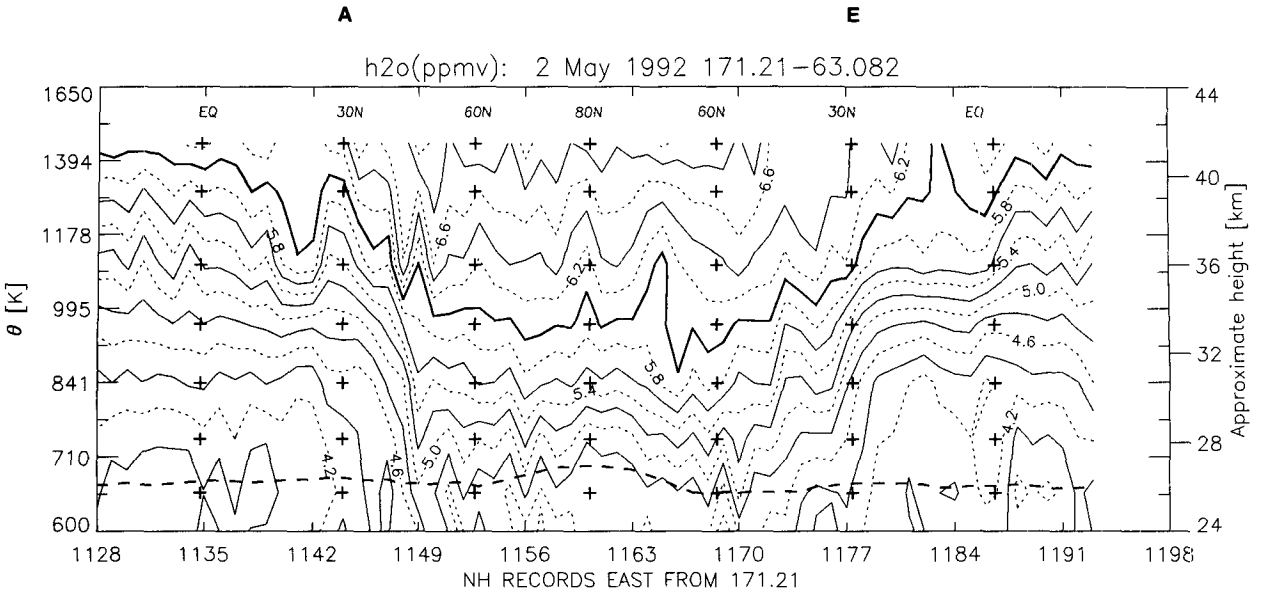

FIG. 18. As Fig. 4 but for MLS water vapor (ppmv) data on 2 May 1992 (*UARS* day 234). The viewing track is from about 20°S, 171°E to 20°S, 63°E. The local solar times are, in ascending record number along the abscissa, approximately 10.3 h (30°N), 17.4 h (80°N), 23.6 h (30°N).

of diabatic descent through isentropic surfaces and quasi-horizontal transport along isentropic surfaces. The distributions of CLAES nitrous oxide, PV, and heating rates also show these clear signatures. The analysis presented in this paper suggests that descent of relatively dry mesospheric air to the midstratosphere is taking place on a timescale of about 4–5 months, in agreement with the analysis of Lahoz et al. (1993).

The results presented in this paper can be summarized in the schematic shown in Fig. 20. In Fig. 20 we can identify the polar vortex (marked *BCD* with *C* its center), the Aleutian high (marked *AB*), a pair of jet

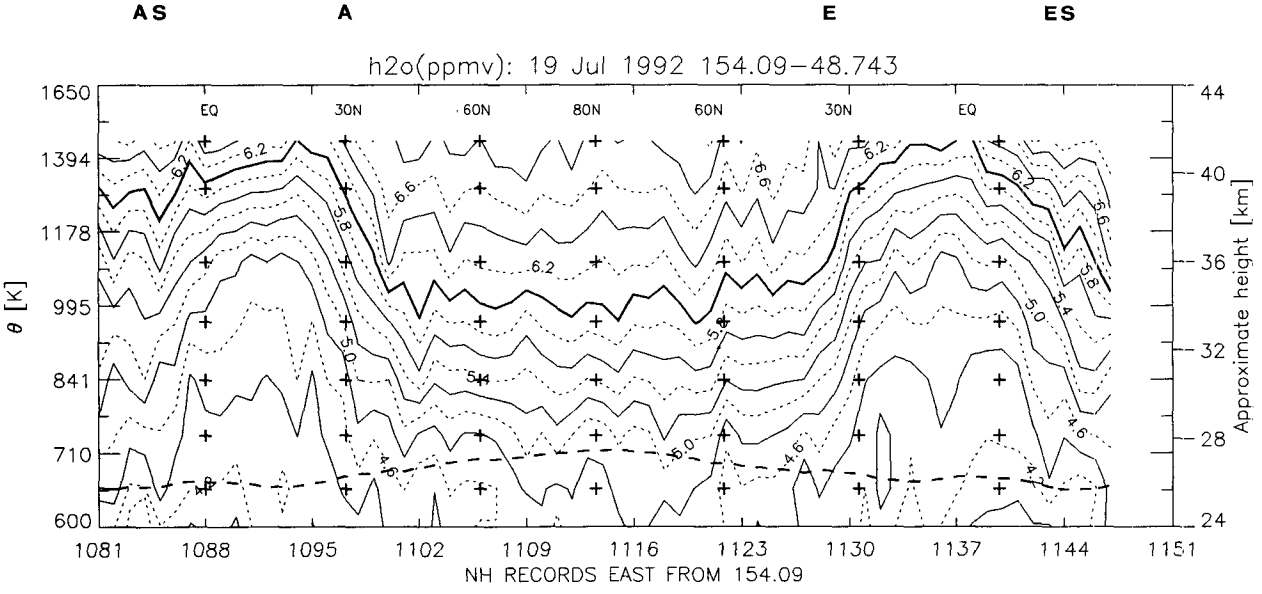

FIG. 19. As Fig. 4 but for MLS water vapor (ppmv) measured on 19 July 1992 (*UARS* day 312). The viewing track is from about 20°S, 154°E to 20°S, 49°E. The local solar times are, in ascending record number along the abscissa, approximately 8.4 h (30°N), 15.1 h (80°N), 21.6 h (30°N).

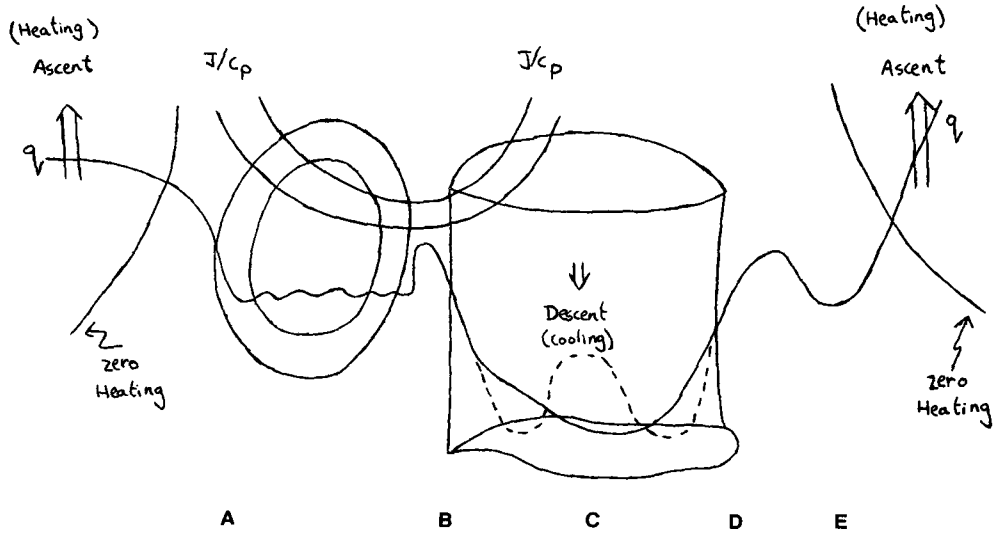

FIG. 20. Typical representation of the northern winter stratosphere vertical cross section. The Aleutian high is marked *AB*; the polar vortex is marked *BCD*, with *C* being the center of the vortex. The region marked *DE* indicates a "ridge" of relatively dry air. The diabatic heating field (marked J/c_p) and a typical isopleth of water vapor (marked q) are superimposed.

streams around the polar vortex (marked *B* and *D*), and a streamer of relatively dry air being advected eastward around the polar vortex (marked *DE*). Note that Fig. 20 is a schematic and is not intended to suggest that the polar vortex has a well-defined edge.

The persistence of strong horizontal gradients in the jet stream around the polar vortex signifies that material lines are aligned with flow lines. Stretching and folding of material in the jet is suppressed by the strong horizontal gradients of PV and, in fact, radial gradients inside the vortex increase with time until the late winter as a result of diabatic descent through isentropic surfaces. This is reflected in the pronounced dip of the water vapor isopleth q (shown in bold in Fig. 20) across the jet streams toward the center of the vortex.

By contrast, in the region of the Aleutian high horizontal gradients of water vapor are not monotonic but change sign over short distances so that, on average, isentropic gradients are much weaker in the Aleutian high than in the polar vortex. The streamer of relatively dry air that is being advected around the vortex is subsequently advected along the jet stream between the polar vortex and the Aleutian high, which accounts for the "ridge" of relatively dry air near *B* in Fig. 20. Trajectory calculations indicate that the streamer ultimately spirals into the anticyclonic circulation associated with the Aleutian high. This coiling up of material lines in the Aleutian high results in air masses with different properties being mixed down to scales below the resolution of instruments such as MLS. Hence, radial gradients are weak in the Aleutian high (apart from structure), and this is reflected in the series of local minima in water vapor mixing ratio interspersed between local maxima across the Aleutian high (marked *AB* in Fig. 20).

The asymmetric heating field J/c_p imposed on the polar vortex and the Aleutian high suggests that the strongest descent, on average, occurs in the Aleutian high and in a ring inside the polar vortex. Given the organization of the large-scale flow by the polar vortex and the Aleutian high, this pattern of descent would lead to filamentary curtains of material extending throughout the depth of the anticyclone and a double peak in the tracer distribution inside the polar vortex (marked by a dashed line at the bottom of the vortex in Fig. 20), as has been seen in high-resolution trajectory studies (V. Pope 1994, personal communication). Neither the filamentary curtains of material nor the double peak in the polar vortex is observed in the water vapor cross sections. This is due to the coarse resolution of the satellite data and/or to stretching and folding of material lines that have weakened the quasi-horizontal gradients. Also, differences between the MLS observations and high-resolution trajectory studies may be due to model deficiencies.

The high quasi-horizontal gradients at *A* and *E* in Fig. 20 are due to a tilting of the water vapor isopleths from the horizontal to the vertical as a consequence of ascent in the upper-stratosphere Tropics and descent in the midlatitude upper stratosphere (note the position of the zero-heating line in Fig. 20). Trajectory calculations indicate that eastward advection, around the vortex, of low-latitude air that is then fed into the anticyclonic circulation of the Aleutian high also contributes toward sharpening the gradients at *A*.

The schematic in Fig. 20, which indicates that the large-scale flow in the winter stratosphere is organized

by the polar vortex and the Aleutian high, has a bearing on issues concerning the nature of the flow in and around the polar vortex (see, e.g., Randel 1993). Similarly, the presence of the high gradients at *A* and *E* in Fig. 20 has a bearing on the stratospheric transport of tropical air to higher latitudes (see, e.g., Randel et al. 1993; Waugh 1993). This transport from the Tropics to midlatitudes is complicated and highly dependent on the quasi-biennial oscillation (QBO) and planetary wave activity. Further work will document the southern winter stratosphere of 1992 by following the structure and evolution of MLS water vapor isopleths in a vortex-centered view.

Acknowledgments. We thank many colleagues who have contributed to the MLS project and in particular to the water vapor measurements: NASA, the *UARS* project office; colleagues at the Jet Propulsion Laboratory, Edinburgh University, Heriot-Watt University, the Rutherford Appleton Laboratory, and the U.K. Meteorological Office; S. Ruth of RAL, V. D. Pope of the UKMO, R. Sutton of Oxford University, and J. Thuburn of CGAM for useful discussions. The work in the United Kingdom was funded by SERC and NERC, and in the United States by NASA.

REFERENCES

Andrews, D. G., J. R. Holton, and C. B. Leovy, 1987: *Middle Atmosphere Dynamics.* Academic Press, 489 pp.

Barath, F. T., and coauthors, 1993: The Upper Atmosphere Research Satellite Microwave Limb Sounder Instrument. *J. Geophys. Res.*, **98,** 10 751–10 762.

Bevilacqua, R. M., J. J. Olivero, P. R. Schwartz, C. J. Gibbins, J. M. Bologna, and D. L. Thacker, 1983: Observational study of water vapor in the mid-latitude mesosphere using ground-based microwave techniques. *J. Geophys. Res.*, **88,** 8523–8534.

Brasseur, G., and S. Solomon, 1984: *Aeronomy of the Middle Atmosphere.* Reidel, 441 pp.

Brewer, A. W., 1949: Evidence for a world circulation provided by the measurements of helium and water vapor distribution in the stratosphere. *Quart. J. Roy. Meteor. Soc.*, **75,** 351–363.

Dobson, G. M. B., 1956: Origin and distribution of polyatomic molecules in the atmosphere. *Proc. Roy. Soc. London,* **A236,** 187–193.

Farman, J. C., B. G. Gardiner, and J. D. Shanklin, 1985: Large losses of total ozone in Antarctica reveal seasonal ClO_x/NO_x interaction. *Nature,* **315,** 207–210.

Fisher, M., A. O'Neill, and R. Sutton, 1993: Rapid descent of mesospheric air into the stratospheric polar vortex. *Geophys. Res. Lett.*, **20,** 1267–1270.

Gunson, M. R., C. B. Farmer, R. H. Norton, R. Zander, C. P. Rinsland, J. H. Shaw, and B.-C. Gao, 1990: Measurements of CH_4, N_2O, CO, H_2O, and O_3 in the middle atmosphere by the Atmospheric Trace Molecule Spectroscopy Experiment on Spacelab 3. *J. Geophys. Res.*, **95,** 13 867–13 882.

Haigh, J. D., 1984: Radiative heating of the lower stratosphere and the distribution of ozone in a two-dimensional model. *Quart. J. Roy. Meteor. Soc.*, **110,** 167–185.

Harwood, R. S., and coauthors, 1993: Springtime stratospheric water vapour in the Southern Hemisphere as measured by MLS. *Geophys. Res. Lett.*, **20,** 1235–1238.

Jones, R. L., J. A. Pyle, J. E. Harries, A. M. Zavody, J. M. Russell III, and J. C. Gille, 1986: The water vapour budget of the stratosphere using LIMS and SAMS satellite data. *Quart. J. Roy. Meteor. Soc.*, **112,** 1127–1143.

Kumer, J. B., J. L. Mergenthaler, and A. E. Roche, 1993: CLAES CH_4, N_2O and CCl_2F_2 (F12) global data. *Geophys. Res. Lett.*, **20,** 1239–1242.

Lahoz, W. A., and coauthors, 1993: Northern Hemisphere mid-stratosphere vortex processes diagnosed from H_2O, N_2O and potential vorticity. *Geophys. Res. Lett.*, **20,** 2671–2674.

——, and coauthors, 1994: Data validation of 183 GHz UARS MLS H_2O measurements. *J. Geophys. Res.*, in preparation.

McIntyre, M. E., and T. N. Palmer, 1983: Breaking planetary waves in the stratosphere. *Nature,* **305,** 593–600.

Olaguer, E. P., H. Yang, and K. K. Tung, 1992: A reexamination of the radiative balance of the stratosphere. *J. Atmos. Sci.*, **49,** 1242–1263.

O'Neill, A., V. D. Pope, W. L. Grose, M. Bailey, H. MacLean, and R. Swinbank, 1994: Evolution of the stratosphere during northern winter 1991/92 as diagnosed from UKMO analyses. *J. Atmos. Sci.*, **51,** 2800–2817.

Randel, W. J., 1993: Ideal flow on Antarctic vortex. *Nature,* **364,** 105–106.

——, J. C. Gille, A. E. Roche, J. B. Kumer, J. L. Mergenthaler, J. W. Waters, E. F. Fishbein, and W. A. Lahoz, 1993: Stratospheric transport from the tropics to middle latitudes by planetary wave mixing. *Nature,* **365,** 533–535.

Reber, C. A., 1993: The Upper Atmosphere Research Satellite (UARS). *Geophys. Res. Lett.*, **20,** 1215–1218.

Remsberg, E. E., J. M. Russell III, and C.-Y. Wu, 1989: An interim reference model for the variability of the middle atmosphere water vapor distribution. *Adv. Space Res.*, **10,** 51–64.

Roche, A. E., J. B. Kumer, J. L. Mergenthaler, G. A. Ely, W. G. Uplinger, J. F. Potter, T. C. James, and L. W. Sterritt, 1993: The Cryogenic Limb Array Etalon Spectrometer (CLAES) on UARS: Experiment description and performance. *J. Geophys. Res.*, **98,** 10 763–10 775.

Russell, J. M., III, A. F. Tuck, L. L. Gordley, J. H. Park, S. R. Drayson, J. E. Harries, R. J. Cicerone, and P. J. Crutzen, 1993: HALOE Antarctic observations in the spring of 1991. *Geophys. Res. Lett.*, **20,** 719–722.

Ruth, S. L., J. J. Remedios, B. N. Lawrence, and F. W. Taylor, 1994: ISAMS measurements of N_2O during the early northern winter 1991/92. *J. Atmos. Sci.*, submitted.

Sutton, R., 1994: Lagrangian flow in the middle atmosphere. *Quart. J. Roy. Meteor. Soc.*, **120,** 1299–1321.

——, H. MacLean, A. O'Neill, R. Swinbank, and F. W. Taylor, 1994: High resolution middle atmosphere tracer fields estimated from satellite observations using Lagrangian trajectory calculations. *J. Atmos. Sci.*, **51,** 2995–3005.

Swinbank, R., and A. O'Neill, 1994: A stratosphere–troposphere data assimilation system. *Mon. Wea. Rev.*, **122,** 686–702.

Waters, J. W., L. Froidevaux, W. G. Read, G. L. Manney, L. S. Elson, D. A. Flower, R. F. Jarnort, and R. S. Harwood, 1993: Stratospheric ClO and ozone from the Microwave Limb Sounder on the Upper Stratosphere Research Satellite. *Nature,* **362,** 597–602.

Waugh, D. W., 1993: Subtropical stratospheric mixing linked to disturbances in the polar vortices. *Nature,* **365,** 535–537.